ORIGINAL PAPER

RJME
Romanian Journal of
Morphology & Embryology
http://www.rjme.ro/

Heterogeneity of human fibroblasts isolated from hypertrophic scar

Raluca Ţuţuianu[1], Ana Maria Roşca[1], Gabriela Florea[1], Vasile Prună[1], Daniela Mădălina Iacomi[1], Luminiţa Andreea Rădulescu[1], Tiberiu Paul Neagu[2,3], Ioan Lascăr[2,3], Irina Domnica Titorencu[1]

[1]"Nicolae Simionescu" Institute of Cellular Biology and Pathology of the Romanian Academy, Bucharest, Romania

[2]Department of Plastic Surgery and Reconstructive Microsurgery, Emergency Clinical Hospital of Bucharest, Romania

[3]Clinical Department No. 11, "Carol Davila" University of Medicine and Pharmacy, Bucharest, Romania

Abstract

Pathological wound healing states, such as hypertrophic scarring and keloids, represent a huge clinical and financial burden on healthcare system. The complex biological mechanisms occurring in hypertrophic scarring are still barely understood. To date, there is no satisfactory description of hypertrophic fibroblasts. Therefore, in the present study we focused on the comparatively characterization of the fibroblasts residing in different regions of hypertrophic scars. To achieve this aim, fibroblasts were isolated from normal skin samples (n=4) and hypertrophic scars (n=4). These cell populations were further were used for the evaluation of proliferation and migration capacity, for the gene and protein expression of extracellular matrix protein type I collagen and fibronectin and for the presence of myofibroblasts. Our results demonstrated that perilesional and intralesional fibroblasts isolated from hypertrophic scars could be considered as distinct populations, having different properties. Thus, the intralesional fibroblasts had an increased proliferation capacity and increased gene and protein expression of collagen I and fibronectin. However, the perilesional fibroblasts had augmented mobility as revealed by *in vitro* scratch test and contained a higher percentage of myofibroblasts [alpha-smooth muscle actin ($α$-SMA)^{high} cells], in comparison to the intralesional population. In conclusion, our data could provide an explanation regarding the inconsistent efficacy of topic therapies for hypertrophic scars.

Keywords: fibroblasts, hypertrophic scars, heterogeneity.

Introduction

The appropriate wound healing is a crucial process, which contributes to the protection of the body from the environmental threats. The formation of a scar is part of the normal mammalian skin repair; however, flows in its dissolution can lead to the formation of pathological scarring, characterized by excessive accumulation of extracellular matrix (ECM) [1]. Thus, the chronic inflammation of the dermis and the abnormal function of myofibroblasts lead to the overgrowth of the scar, resulting in a hypertrophic or a keloid scar [2]. Although they share some similar traits, hypertrophic and keloid scars have a different etiology and distinct structural and molecular characteristics [1]. While the keloid scars represent a complex fibro-proliferative disorder of the skin, which spreads beyond the borders of the original injury and frequently recurs after excision [3], hypertrophic scars are confined inside the limits of the original injury, they may flatten over several years and they do not reappear once removed [4]. The development of hypertrophic scars is a common abnormal result following surgery (40% to 70%) and up to 91% subsequent to burn injury [5]. Individuals having hypertrophic scars suffer pain, pruritus and even loss of joint mobility, function of the injured limb or anatomical defects, which negatively impact their quality of life and their integration in society, posing in the same time a huge financial burden on the healthcare system [6]. It was demonstrated that aberrant fibroblast phenotype seems to

contribute to the hypertrophic scars or post-burn scars [7]. Several treatments have been established for hypertrophic scars, among which corticosteroid injections, splinting and pressure therapy, interferon and 5-Fluorouracil therapy and surgical excision [8]. However, these therapeutic strategies are not entirely successful and there is no agreement regarding the most effective treatment to lastingly improve scars, while having negligible side effects [9]. The scars following burn injuries are most challenging, often being surgically removed in order to regain mobility or for esthetic reasons [10]. Therefore, a novel treatment, based on a specific molecular or cellular target, would have a major impact on the life of many patients. However, for this purpose, additional studies on the scar physiology are needed, leading to the identification of suitable therapeutic targets.

Fibroblasts, as main cellular component in the connective tissue, are critical participants to the wound healing process [11]. However, the fibroblasts inside a scar are metabolically different from their extralesional counterparts [12]. Moreover, it has been shown that the fibroblasts inside the keloid scar are heterogeneous and they have different properties depending on their localization in the tissue. Thus, perilesional fibroblasts have higher proliferation rates, they are more metabolically active and they produce higher quantities of collagen I and III compared to the intralesional fibroblasts, localized in the central area of the scar [13]. Nevertheless, there is little available data regarding the heterogeneity of fibroblasts in the hypertrophic scars.

Therefore, the aim of this study was to comparatively characterize the fibroblasts residing in different regions of hypertrophic scars.

Patients, Materials and Methods

Fibroblasts isolation

Dermal fibroblasts were isolated from human skin samples obtained either from normal mammary samples (*n*=4) from plastic surgery procedures of from patients who underwent plastic surgery to correct excess hypertrophic scar tissue. All the procedures were approved by the Institutional Ethical Committee (No. 180/27.09.2018), in accordance to the most recent version of the Helsinki Declaration of *World Medical Association* (Ethical Principles for Medical Research Involving Human Subjects, October 2008). All samples employed in the study were obtained from biopsies taken from different anatomical locations. Before collecting the samples, written informed consent was obtained from the patients. All scars used were at least 10-year-old. The scars were divided into perilesional (*n*=4) and intralesional (*n*=4), as shown in Figure 1.
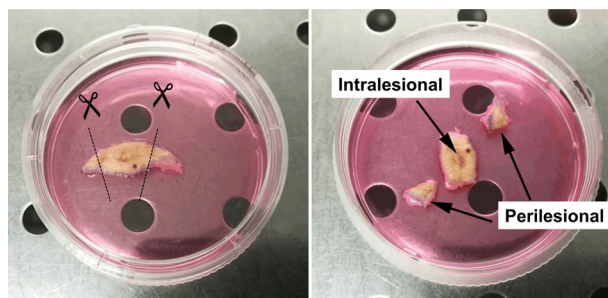

Figure 1 – *Schematic representation of excised hypertrophic scars splitting for explant preparation. Surgically excised tissue was divided into intralesional (central area) and perilesional (marginal areas) tissue pieces.*

Thus, the outer margins were cut with the scissors and considered perilesional, while the center was termed intralesional. The tissue was either processed for histology assessment and immunohistochemistry (IHC), or used for isolation of fibroblasts by explant method, which were multiplied in low glucose Dulbecco's modified Eagle medium (DMEM) supplemented with 15% fetal bovine serum (FBS), at 37°C and 5% CO_2. When confluent, the cells were detached using 0.125% trypsin supplemented with 0.5 mM ethylenediaminetetraacetic acid (EDTA) and seeded at 10 000 cells/cm^2 for further expansion. Dermal fibroblasts from passage 2–3 were used for the experiments.

Histology and immunohistochemistry

Skin fragments were either fixed in formalin, followed by dehydration in 70%, 90% and 100% ethanol, clearing in xylene and infiltration for paraffin embedding or freshly frozen in optimal cutting temperature (OCT) compound for cryosectioning. Histological staining [Hematoxylin–Eosin (HE) and Herovici's] was performed on 5 μm paraffin sections. For the Herovici staining, after rehydration, the slides were maintained in Weigert's iron Hematoxylin for 5 minutes, followed by a tap water rinse and the staining solution consisting of 1% Acid Fuchsin in saturated picric acid solution, 0.05% Aniline Blue, glycerol, and saturated lithium carbonate for 5 minutes. After a 2 minutes wash in 1% acetic acid, the sections were dehydrated with

ethanol, cleared in xylene, mounted with glycerol and examined using a Zeiss Observer D1 microscope. IHC was performed on 5 μm cryosections fixed in methanol. Briefly, after blocking in 1% gelatin, the following antibodies were used: anti-cluster of differentiation 45 (CD45)–fluorescein isothiocyanate (FITC) (BioLegend), anti-alpha-smooth muscle actin (*α*-SMA) (Invitrogen), anti-type I collagen and anti-type III collagen (both from ThermoFisher Scientific). Depending on the primary antibody, either anti-mouse Alexa 568 or anti-rabbit Alexa 488 secondary antibody (both from ThermoFisher Scientific) were used. The nuclei were stained with 4',6-diamidino-2-phenylindole (DAPI) (Sigma-Aldrich), and after mounting with ProLong® Gold (ThermoFisher Scientific), the slides were examined using a Zeiss Observer D1.

Immunocytochemistry

Fibroblasts were grown in 24-well plates on glass coverslips and fixed in 4% paraformaldehyde (PFA). After permeabilization with 0.1% Triton X, the cells were rinsed with phosphate-buffered saline (PBS) and stained with the following antibodies: anti-type I collagen (ThermoFisher Scientific), anti-vimentin (Sigma-Aldrich), anti-*α*-SMA (Invitrogen) and anti-fibronectin (ThermoFisher Scientific). For the secondary antibodies, anti-mouse Alexa 568 or anti-rabbit Alexa 488 secondary antibody (both from ThermoFisher Scientific) were used. After three washes in PBS, the coverslips were mounted with Fluoroshield™ with DAPI (Sigma-Aldrich) and examined using a Zeiss Observer D1.

xCELLigence assay

The proliferation of fibroblasts isolated from hypertrophic scars *versus* normal fibroblasts was evaluated with xCELLigence System (ACEA Biosciences, Inc.), which monitors cellular events in real time by measuring electrical impedance across interdigitated microelectrodes integrated on the bottom of tissue culture E-plates. Briefly, the cells were seeded on E-plates in serum-containing DMEM at a density of 3000 cells/well; cellular index was monitored for 125 hours. The normalization of cellular index was performed t=4 hours, after the cells have adhered to the culture substrate.

Wound healing assay

Ten thousand extralesional, intralesional and perilesional fibroblasts (passage 2) were seeded in 96-well plate and incubated in complete culture medium for 24 hours. After 24 additional hours of starvation (low glucose DMEM supplemented with 0.5% FBS), the monolayer was scratched transversely in the middle of the well using a 200-μL pipette tip, washed with PBS and incubated in complete culture medium. To assess the extent of migration, the cells were photographed immediately after the addition of the media (t=0 hours) and then at t=18 hours. The migration of the cells into the scratched area was assessed by measuring the area covered by cells using ImageJ software (NIH).

Real-time polymerase chain reaction (PCR)

Total ribonucleic acid (RNA) was extracted using the TRIzol reagent (ThermoFisher Scientific) and complementary deoxyribonucleic acid (cDNA) was synthesized starting

from 1 μg of total RNA employing High-Capacity cDNA Reverse Transcription Kit (Applied Biosystems). Real-time PCR was performed using The SensiFAST™ SYBR Hi-ROX Kit (Bioline) optimized amplification conditions. The primer sequences are available upon request. The analysis was done using the comparative CT method and β-actin was employed for internal normalization.

Western blot

Cells were washed with PBS and scraped off in hot Laemmli's loading buffer (Sigma-Aldrich). Equal amounts of protein extracts (20 μg/lane) were separated by sodium dodecyl sulfate (SDS)–polyacrylamide gel electrophoresis (PAGE) and transferred on nitrocellulose membrane (Bio-Rad). After blocking in Tris-buffered saline (TBS) containing 0.05% Triton X-100 and 5% milk for one hour, the membranes were incubated with the corresponding primary antibodies [mouse anti-α-SMA (eBioscience), mouse anti-β-actin (Sigma-Aldrich), rabbit anti-collagen I, mouse anti-collagen III and rabbit anti-fibronectin (all from ThermoFisher Scientific)] overnight, at 4°C, washed and then incubated with the secondary antibody (anti-mouse and anti-rabbit, all from ThermoFisher Scientific) labeled with horseradish peroxidase (HRP) for one hour, at room temperature. Antigen–antibody complexes were visualized through chemiluminescence by using an ECL kit (Millipore).

Flow cytometry

Cells at passage 2 were detached with trypsin (Sigma-Aldrich), fixed with 4% PFA for 10 minutes/37°C and then with methanol 10 minutes on ice. Next, fibroblasts were incubated with mouse anti-α-SMA (eBioscience) for 30 minutes/room temperature and then with secondary anti-mouse immunoglobulin G (IgG) AlexaFluor 568 (Life Technologies) for another 30 minutes/room temperature. After three washing steps, the samples containing 10^5 cells were analyzed using a Beckman Coulter 3 laser CytoFLEX flow cytometer and the data were analyzed with Summit software v4.3 (Cytomation, Inc.).

Gel contraction assay

The assay was performed in 24-well plates, using a final volume of 500 μL per well, consisting of 66% fibroblasts suspension in culture medium (150 000 cell/mL)

and 33% of type I rat tail collagen (3 mg/mL, Merck Millipore) and the adequate volume of 1M sodium hydroxide needed to turn the color from yellow to slightly pink. After the collagen solidified, the gel was carefully detached from the well and 500 μL of culture medium was added. Pictures for each well were taken after medium addition (t0) and after 24 hours (tf). Using Image J software, the initial (A0) and final area (Af) were quantified, and the contraction capacity of the fibroblasts was expressed as follows: (A0–Af)/A0×100.

Statistical analysis

Data were analyzed with GraphPad Prism 5.0 (GraphPad Software, Inc.) and presented as mean ± standard deviation (SD) of representative experiments. Comparison of multiple groups was done by analysis of variance (ANOVA). Two-group analysis was carried out by Student's t-test. Probability values less than 0.05 were considered significant (* – $p<0.05$, ** – $p<0.01$, *** – $p<0.001$, ns – not significant).

⊟ Results

Histological evaluation of hypertrophic scars

The histological aspect of the scar tissue corresponding to the intra- and perilesional areas, in comparison to the normal/extralesional tissue, can be observed in Figure 2. Thus, the flattened epidermis and the arrangement of collagen fibers in clusters parallel to the epidermis were observed in the intralesional (center), as well as in the perilesional area (periphery). Moreover, the HE staining showed a rich inflammatory infiltrate, which was noticed both in the intra- and perilesional areas. The extravasation of inflammatory cells was also showed by IHC. In Figure 3, CD45-positive cell can be noticed outside the blood vessel area, labeled by α-SMA staining.

The expression and arrangement of collagen type I and type III fibers were showed by Herovici staining (collagen III fibers stained in blue and collagen I fibers stained in red) and in parallel with IHC. Thus, Figure 4 shows the more abundant presence of collagen III, oriented parallel to the epidermal surface, in scar tissue, both in intra- and perilesional areas, in comparison to normal tissue.
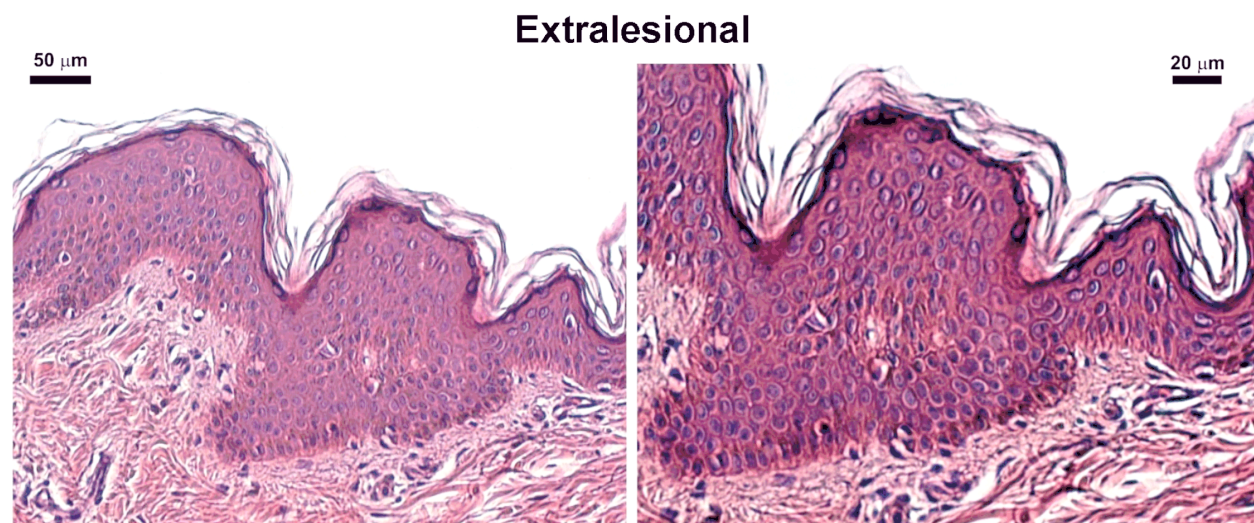
Extralesional

Figure 2 – *Comparative histological evaluation of normal versus hypertrophic scars biopsies by Hematoxylin–Eosin (HE) staining.*

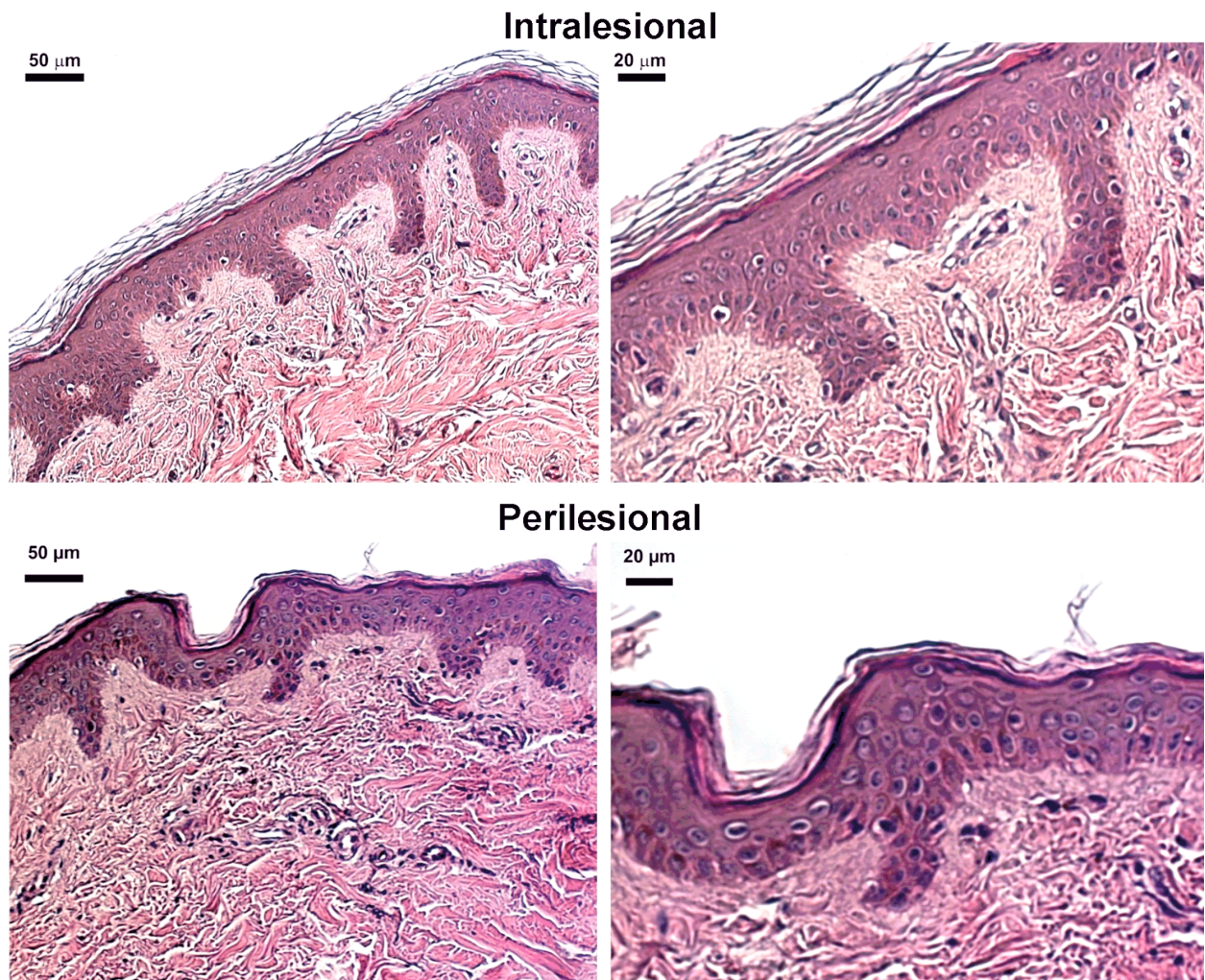## Intralesional

Perilesional

Figure 2 (continued) – *Comparative histological evaluation of normal versus hypertrophic scars biopsies by Hematoxylin– Eosin (HE) staining.*
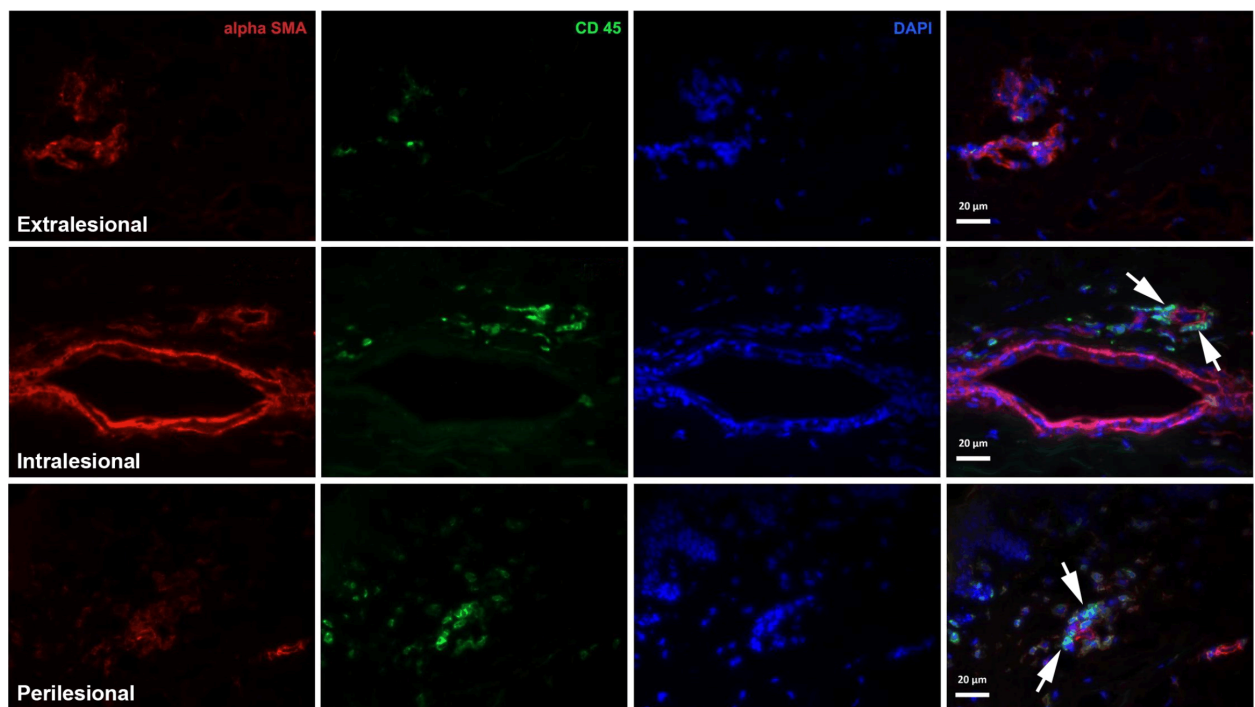

Figure 3 – *Comparative immunohistochemical assessment of the perivascular inflammatory infiltrate in intralesional and perilesional regions of the hypertrophic scars versus normal skin. CD45: Cluster of differentiation 45; DAPI: 4',6-Diamidino-2-phenylindole; α-SMA: Alpha-smooth muscle actin.*
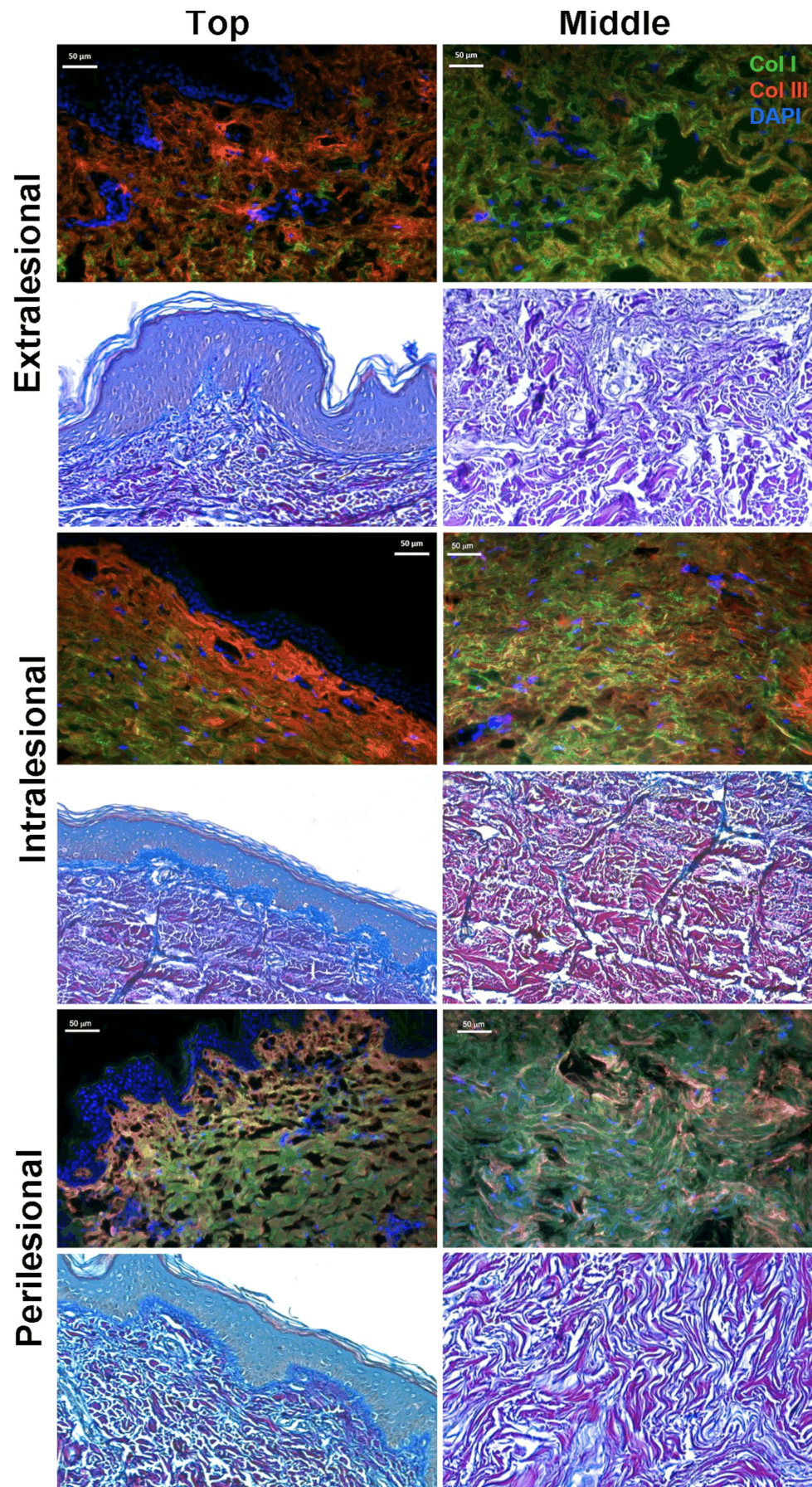
Figure 4 – *Assessment of localization and arrangement of Col I and Col III fibers in intralesional and perilesional areas of the hypertrophic scars versus normal skin by Herovici staining and immunohistochemistry. In Herovici staining, young collagen and reticulin are shown in blue and mature collagen in red. Col I: Collagen I; Col III: Collagen III; DAPI: 4',6-Diamidino-2-phenylindole.*

Evaluation of proliferation and migration capacity

The fibroblasts isolated from the scar explants exhibited the characteristic spindle-shaped morphology, as shown in Figure 5a. The proliferative capacity of hypertrophic scar fibroblasts was estimated by xCELLIgence assay. In Figure 5b, the increased proliferative capacity of both types of scar fibroblasts in contrast to normal extralesional cells can be observed. However, a significant difference between the proliferation of intra- *versus* perilesional fibroblasts was noticed. Thus, the cellular index of intralesional fibroblasts measured after five days in culture was 1.5 times higher than the index of perilesional fibroblasts and two times higher than the index of normal fibroblasts. Next, we evaluated the capacity of migration of the three cell types by *in vitro* scratch test. Consistently with the proliferation data, the results indicated stronger migration ability for scar fibroblasts in comparison to normal fibroblasts. However, the perilesional cells covered 76% of scratched area, in comparison to 65% and 45% in the cases of intralesional and normal fibroblasts, respectively (Figure 5c). Consequently, although scar fibroblasts had increased proliferative and migratory properties in comparison to normal fibroblasts, a significant difference between these abilities in relation to their localization within the scar was observed. Thus, the intralesional/central fibroblasts were highly proliferative, while the perilesional/marginal fibroblasts had increased migration capacity.

Assessment of type I and type III collagen expression by hypertrophic scar fibroblasts

The increased collagen production in hypertrophic scars is well established; however, we asked the question whether the capacity of collagen synthesis of fibroblasts residing in hypertrophic scars varies according to their location within the tissue. The increased expression of collagen I by scar fibroblasts was easily noticed, as shown by the immunocytochemistry images in Figure 6a. Nevertheless, the real-time PCR experiments showed that the gene expression of collagen I was up to two folds increased in intralesional fibroblasts, in comparison to normal and intralesional cells (Figure 6b), while the protein expression, as shown by Western blot assay in Figure 6c, did not indicate a major difference between the two populations of scar fibroblasts.
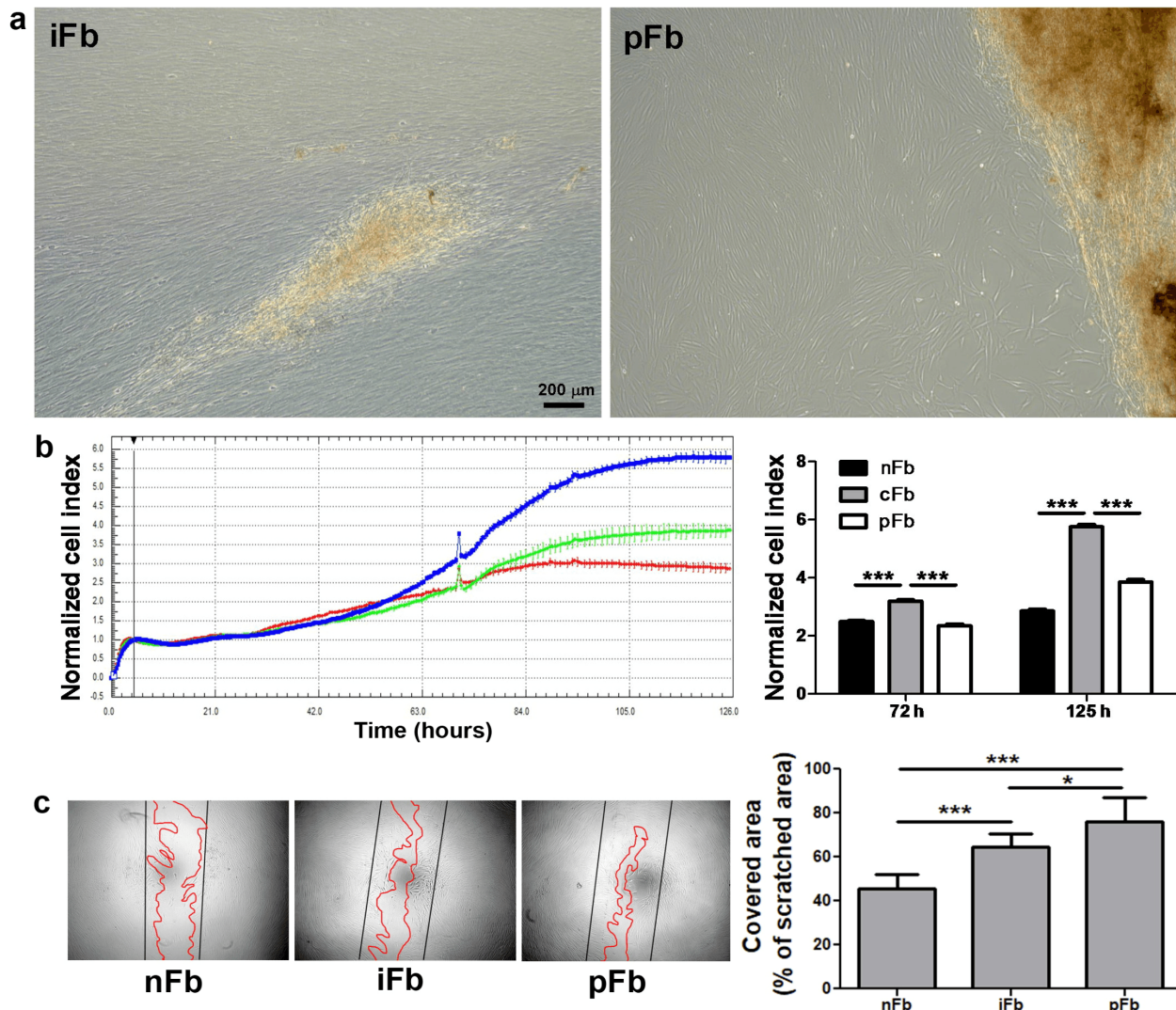

Figure 5 – *Evaluation of normal, intralesional and perilesional hypertrophic fibroblasts properties: (a) Phase contrast microscopy pictures depicting scar-derived fibroblasts spindle-shape morphology; (b) Real-time monitoring of cell proliferation by xCELLigence technique (the diagram on the right illustrates the cellular index at 72 versus 125 hours); (c) Scratch test assay of fibroblasts migration capacity. cFb: Central fibroblasts; iFb: Intralesional fibroblasts; nFb: Normal fibroblasts; pFb: Perilesional fibroblasts. *p<0.05, ***p<0.001.*
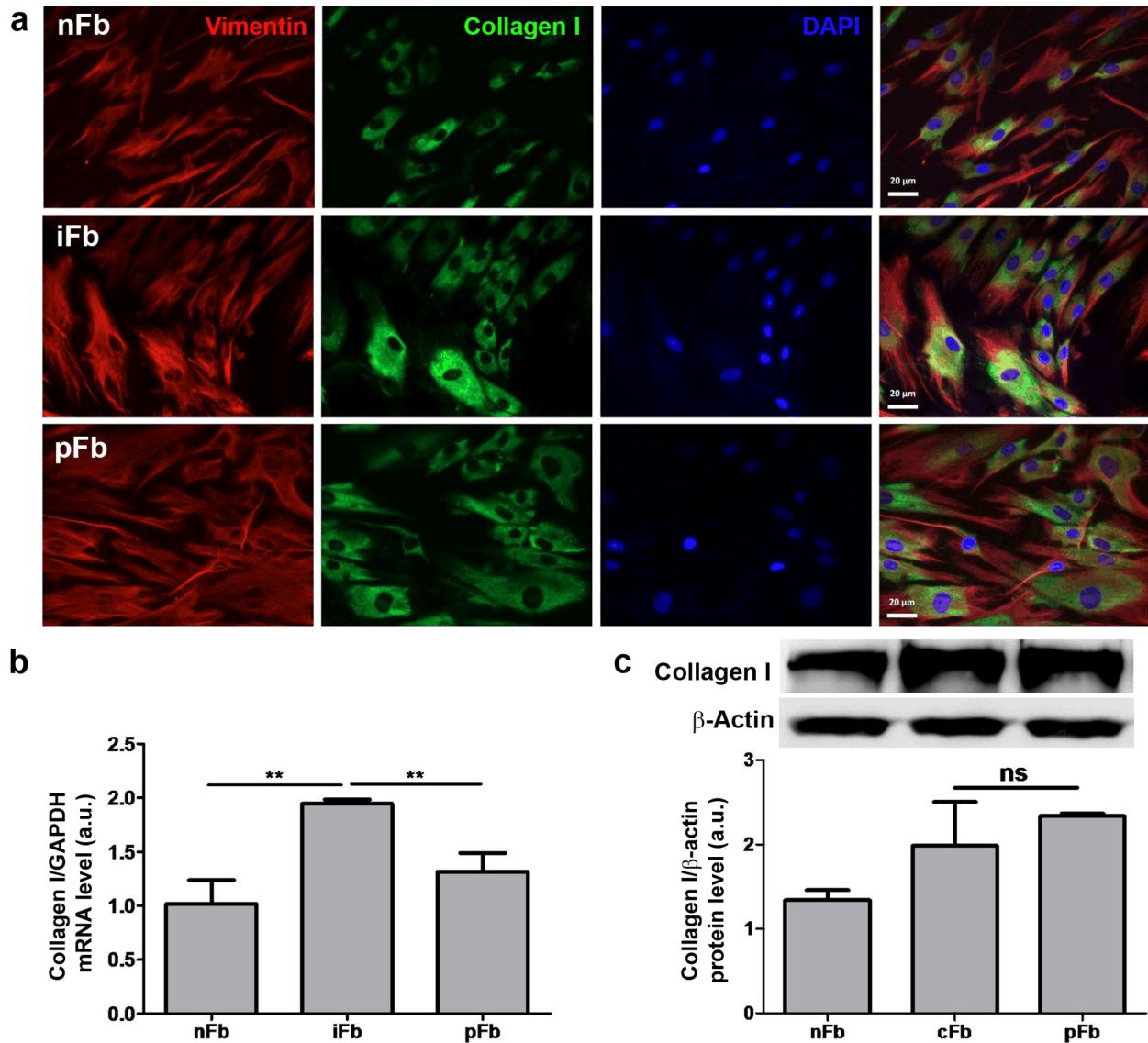
Figure 6 – *Evaluation of type I collagen expression in scar versus normal fibroblasts: (a) Immunocytochemical staining showing the presence of collagen I versus vimentin; (b) Gene expression of type I collagen measured by real-time PCR; (c) Protein expression of type I collagen revealed by Western blot technique. a.u.: Arbitrary units; DAPI: 4',6-Diamidino-2-phenylindole; cFb: Central fibroblasts; iFb: Intralesional fibroblasts; nFb: Normal fibroblasts; pFb: Perilesional fibroblasts; GAPDH: Glyceraldehyde 3-phosphate dehydrogenase; mRNA: Messenger ribonucleic acid; PCR: Polymerase chain reaction. **p<0.01, ns: Not significant.*

Assessment of fibronectin expression by hypertrophic scar fibroblasts

An abnormal amount of fibronectin is a hallmark of pathological scars [14], therefore we checked the expression of this ECM component by the two scar fibroblasts populations in comparison to normal fibroblasts. As shown by immunocytochemistry in Figure 7a, both populations of scar-derived fibroblasts were intensively positive for fibronectin. The quantification of gene expression by real-time PCR indicated the highest fibronectin expression by intralesional fibroblasts, up to two folds higher in comparison to normal and perilesional fibroblasts (Figure 7b). However, the protein expression of fibronectin by cultured fibroblasts, as estimated by Western blot technique (Figure 7c), indicated only a minor difference between the three cell populations. Nevertheless, the protein expression of fibronectin was highest in intralesional fibroblasts.

Assessment of α-SMA expression by hypertrophic scar fibroblasts

Next, we checked the expression of α-SMA, an important marker for myofibroblasts. As shown in Figure 7a, the gene expression was two and 1.7 folds higher in intralesional *versus* normal fibroblasts and perilesional fibroblasts, respectively. However, the protein expression of α-SMA, as revealed by Western blot (Figure 7b) was higher in perilesional fibroblasts in comparison to normal and intralesional fibroblasts, which suggested the presence of myofibroblasts. Therefore, we verified the organization of α-SMA in stress fibers, characteristic for contractile myofibroblasts by immunocytochemistry and flow cytometry. The immunocytochemistry data indicated that cells having organized stress fibers were found mostly in scar-derived rather than in normal fibroblasts (Figure 7c). While the quantification of myofibroblasts in the cultured cell populations by flow cytometry showed an increased

number of α-SMA^{high} cells in both intra- and perilesional populations (Figure 7d), the percentage of α-SMA^{high} cells was 1.6 times higher in the perilesional *versus* intralesional fibroblasts, suggesting the preferential accumulation of these cells in the marginal area of the scar. Given the fact that myofibroblasts are responsible for scar contracture, we tested this feature by embedding normal, intra- and perilesional fibroblasts into collagen gels, in order to measure their contraction capacity. The results indicated an increased capacity of contraction for the scar fibroblasts (more than 60% contraction in 24 hours) in comparison to normal cells (50% contraction in 24 hours). Although the perilesional fibroblasts induced a slightly higher contraction of the collagen gel in comparison to the intralesional fibroblasts (67% *versus* 63%, respectively), there was no statistical relevance (Figure 8, a–e).

⊡ Discussions

Dermal fibroblasts are crucial components of the skin, implicated in producing and organizing the ECM of the dermis, but also in communication with other cell types, playing a central role in regulating skin physiology [15]. Various studies gave rise to the concept of heterogeneity of fibroblasts, stating that this type of cell is represented by multiple distinct subpopulations, having different properties, according to their body site and spatial location [16]. This could have important consequences for the understanding of a numerous pathological conditions, such as scarring, cancer and chronological aging [17] and could lead to the innovation of novel therapies. Nevertheless,

various studies showed that the function of fibroblasts is altered in different pathologies. Thus, in chronic non-healing wounds, fibroblasts are senescent, have decreased proliferation, they display an altered panel of cytokine secretion and abnormal metalloproteinases activity [18–20]. On the other hand, keloid fibroblasts have increased proliferation and decreased apoptosis [21], while the hypertrophic scar-derived fibroblasts have been suggested to closely resemble fibroblasts from deeper dermal layers [22].

The heterogeneity of fibroblasts among the keloid scar is well documented. Thus, it was shown that marginal fibroblasts are more metabolically active and produce higher rates of collagen I and III [15]. Moreover, it was demonstrated that site-specific keloid fibroblasts induce an abnormal phenotype in surrounding quiescent fibroblasts *via* paracrine signaling [23]. However, little is known about the subpopulations of fibroblasts residing in the hypertrophic scars. In this study, we aimed to verify whether the fibroblasts isolated from the marginal/perilesional regions of the hypertrophic scar differ in terms of proliferation capacity, ECM production and differentiation towards the myofibroblast phenotype from their counterparts isolated from the central/intralesional area. Our data indicated that, indeed, perilesional and intralesional fibroblasts isolated from hypertrophic scars could be considered as distinct populations, having different properties. Thus, the intralesional fibroblasts had an increased proliferation capacity and increased gene and protein expression of collagen I and fibronectin.
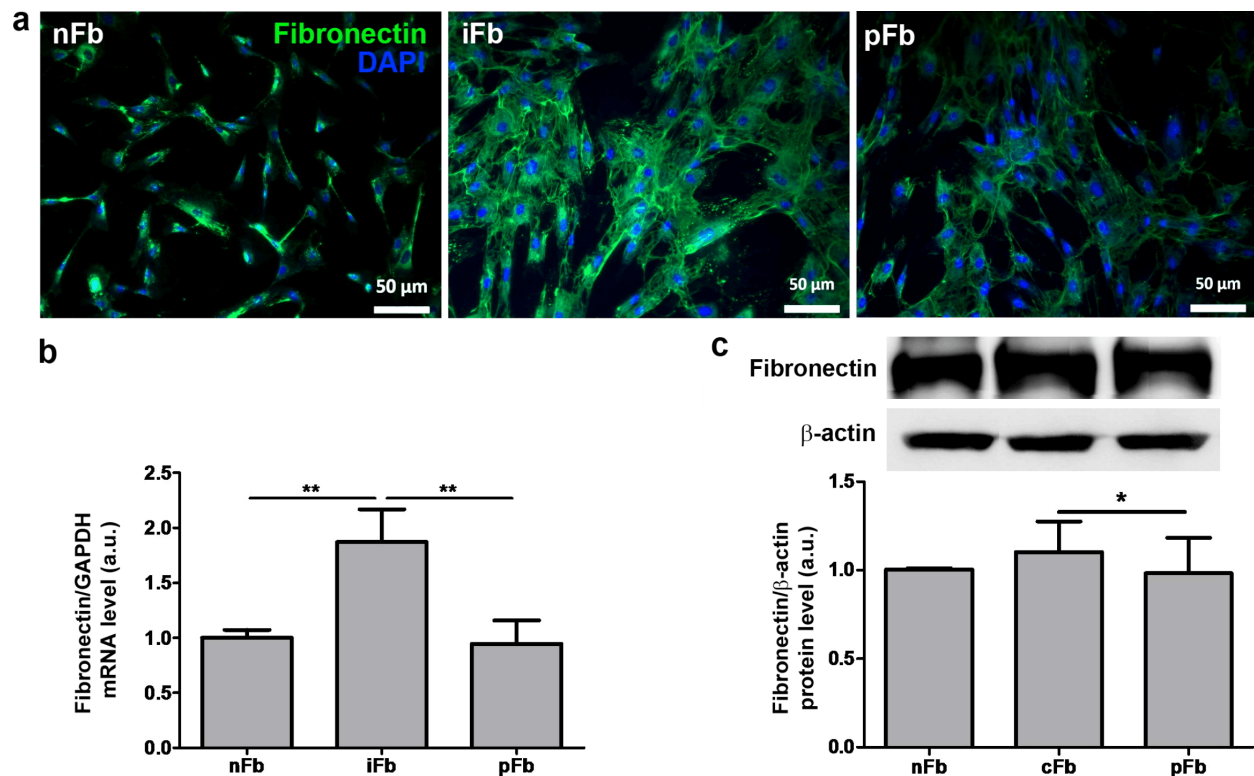

Figure 7 – *Evaluation of fibronectin expression in scar versus normal fibroblasts: (a) Immunocytochemical staining showing the presence fibronectin in primary cultures of normal versus scar-derived fibroblasts; (b) Gene expression of fibronectin measured by real-time PCR; (c) Protein expression of fibronectin revealed by Western blot technique. a.u.: Arbitrary units; DAPI: 4',6-Diamidino-2-phenylindole; cFb: Central fibroblasts; iFb: Intralesional fibroblasts; nFb: Normal fibroblasts; pFb: Perilesional fibroblasts; GAPDH: Glyceraldehyde 3-phosphate dehydrogenase; mRNA: Messenger ribonucleic acid; PCR: Polymerase chain reaction. *p<0.05, **p<0.01.*
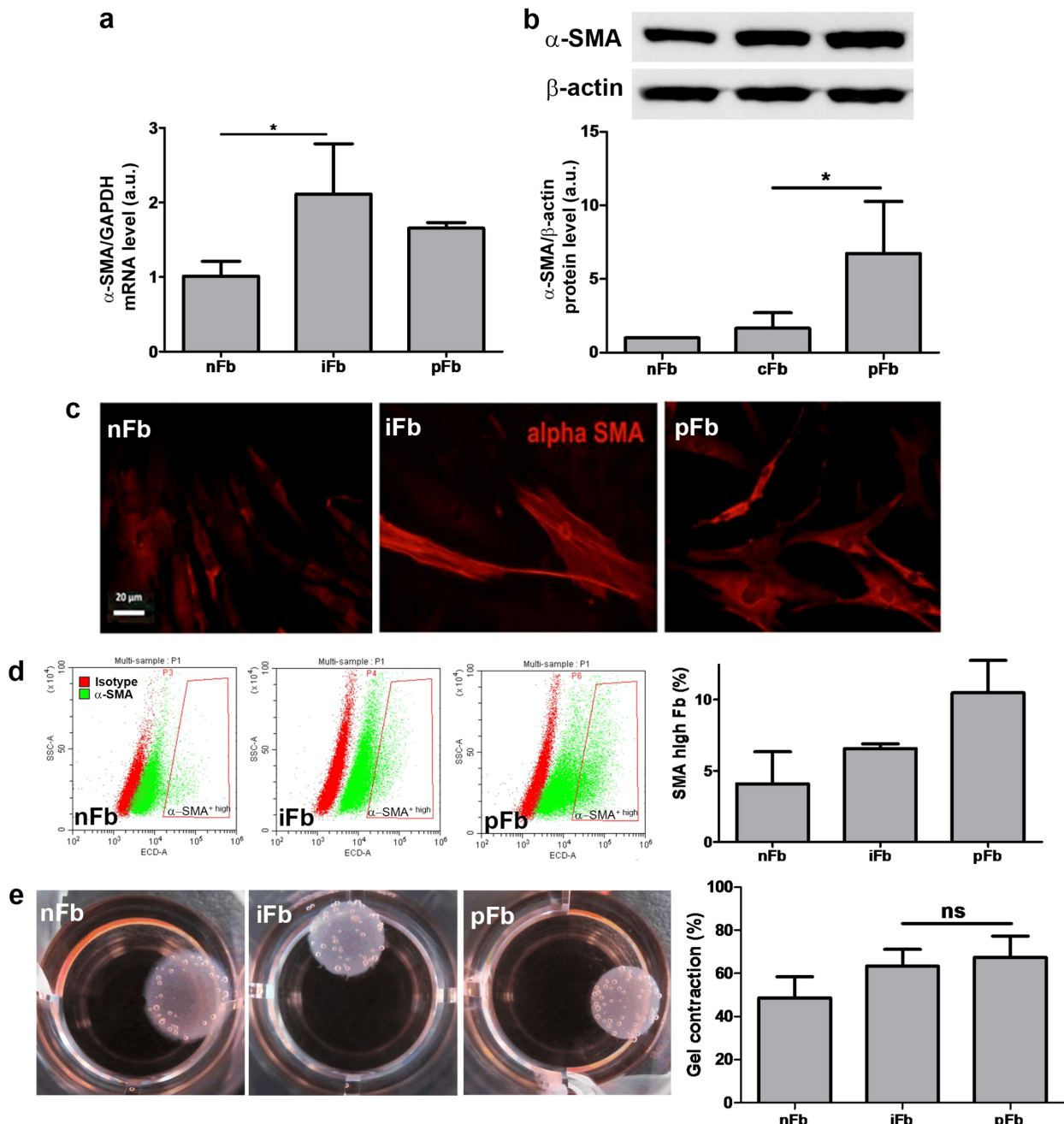
Figure 8 – *Assessment α-SMA expression in normal, intralesional and perilesional hypertrophic fibroblasts: (a) Gene expression of α-SMA measured by real-time PCR; (b) Protein expression of α-SMA revealed by Western blot technique; (c) Immunocytochemical staining showing the organization of α-SMA in stress fibers; (d) Evaluation of α-SMA-positive cells/myofibroblasts in the three examined fibroblast populations by flow cytometry; (e) Estimation of cell contractibility by gel contraction assay. α-SMA: Alpha-smooth muscle actin; a.u.: Arbitrary units; cFb: Central fibroblasts; iFb: Intralesional fibroblasts; nFb: Normal fibroblasts; pFb: Perilesional fibroblasts; GAPDH: Glyceraldehyde 3-phosphate dehydrogenase; mRNA: Messenger ribonucleic acid; PCR: Polymerase chain reaction. *p<0.05, ns: Not significant.*

However, the perilesional fibroblasts had augmented mobility as revealed by *in vitro* scratch test and contained a higher percentage of myofibroblasts (α-SMA^high cells), generally accepted as permanently present in hypertrophic scars [24–26] in comparison to the intralesional population. Although the *in vitro* testing of their contracting capacity was not statistically significant, the presence of an increased percentage of myofibroblasts could translate *in vivo* in an amplified participation to the scar contracture. Moreover, the presence of a larger number of myofibroblasts in the perilesional population could explain also the increased migration capacity.

Our results suggest that, unlike the keloid fibroblasts, which are more active at the margins, in hypertrophic scars, an attenuation of the hypertrophic character from the center to the periphery could occur. However, the presence of myofibroblasts that are mainly located at the edge of the scarring could be an exception from this tendency, contributing to the contracture of the scar margins. This study may help in understanding the pathogenesis of hypertrophic lesions, their differentiation, interpretation of the clinical behavior and planning the appropriate management of abnormal scar and avoid its recurrence.

⊡ Conclusions

Our result indicated that the populations of hypertrophic scar-derived fibroblasts have different properties dependent of localization within the marginal or central areas of the scar. Our data could provide an explanation regarding the inconsistent efficacy of topic therapies for hypertrophic scars. Furthermore, one could safely assume that additional studies, regarding their specific pathways, should be performed, in order to identify precise therapeutic targets for each cell population located within the scar.

Conflict of interests
The authors declare no conflict of interests.

Authors' contribution
Raluca Ţuţuianu and Ana Maria Roşca equally contributed to the manuscript.

Acknowledgments

References

[1] Karppinen SM, Heljasvaara R, Gullberg D, Tasanen K, Pihlajaniemi T. Toward understanding scarless skin wound healing and pathological scarring. F1000Res, 2019, 8:F1000 Faculty Rev-787.

[2] Hinz B. The role of myofibroblasts in wound healing. Curr Res Transl Med, 2016, 64(4):171–177.

[3] Shih B, Garside E, McGrouther DA, Bayat A. Molecular dissection of abnormal wound healing processes resulting in keloid disease. Wound Repair Regen, 2010, 18(2):139–153.

[4] Berman B, Maderal A, Raphael B. Keloids and hypertrophic scars: pathophysiology, classification, and treatment. Dermatol Surg, 2017, 43(Suppl 1):S3–S18.

[5] Gauglitz GG, Korting HC, Pavicic T, Ruzicka T, Jeschke MG. Hypertrophic scarring and keloids: pathomechanisms and current and emerging treatment strategies. Mol Med, 2011, 17(1–2):113–125.

[6] Chiang RS, Borovikova AA, King K, Banyard DA, Lalezari S, Toranto JD, Paydar KZ, Wirth GA, Evans GR, Widgerow AD. Current concepts related to hypertrophic scarring in burn injuries. Wound Repair Regen, 2016, 24(3):466–477.

[7] Song R, Bian HN, Lai W, Chen HD, Zhao KS. Normal skin and hypertrophic scar fibroblasts differentially regulate collagen and fibronectin expression as well as mitochondrial membrane potential in response to basic fibroblast growth factor. Braz J Med Biol Res, 2011, 44(5):402–410.

[8] O'Leary R, Wood EJ, Guillou PJ. Pathological scarring: strategic interventions. Eur J Surg, 2002, 168(10):523–534.

[9] Liu BH, Chen L, Li SR, Wang ZX, Cheng WG. Smac/DIABLO regulates the apoptosis of hypertrophic scar fibroblasts. Int J Mol Med, 2013, 32(3):615–622.

[10] Bombaro KM, Engrav LH, Carrougher GJ, Wiechman SA, Faucher L, Costa BA, Heimbach DM, Rivara FP, Honari S. What is the prevalence of hypertrophic scarring following burns? Burns, 2003, 29(4):299–302.

[11] Kwan P, Hori K, Ding J, Tredget EE. Scar and contracture: biological principles. Hand Clin, 2009, 25(4):511–528.

[12] Nedelec B, Shankowsky H, Scott PG, Ghahary A, Tredget EE. Myofibroblasts and apoptosis in human hypertrophic scars: the effect of interferon-alpha2b. Surgery, 2001, 130(5):798–808.

[13] Tan S, Khumalo N, Bayat A. Understanding keloid pathobiology from a quasi-neoplastic perspective: less of a scar and more of a chronic inflammatory disease with cancer-like tendencies. Front Immunol, 2019, 10:1810.

[14] Ishise H, Larson B, Hirata Y, Fujiwara T, Nishimoto S, Kubo T, Matsuda K, Kanazawa S, Sotsuka Y, Fujita K, Kakibuchi M, Kawai K. Hypertrophic scar contracture is mediated by the TRPC3 mechanical force transducer *via* NFκB activation. Sci Rep, 2015, 5:11620.

[15] Sorrell JM, Caplan AI. Fibroblast heterogeneity: more than skin deep. J Cell Sci, 2004, 117(Pt 5):667–675.

[16] Ali-Bahar M, Bauer B, Tredget EE, Ghahary A. Dermal fibroblasts from different layers of human skin are heterogeneous in expression of collagenase and types I and III procollagen mRNA. Wound Repair Regen, 2004, 12(2):175–182.

[17] Lynch MD, Watt FM. Fibroblast heterogeneity: implications for human disease. J Clin Invest, 2018, 128(1):26–35.

[18] Wall IB, Moseley R, Baird DM, Kipling D, Giles P, Laffafian I, Price PE, Thomas DW, Stephens P. Fibroblast dysfunction is a key factor in the non-healing of chronic venous leg ulcers. J Invest Dermatol, 2008, 128(10):2526–2540.

[19] Cook H, Davies KJ, Harding KG, Thomas DW. Defective extracellular matrix reorganization by chronic wound fibroblasts is associated with alterations in TIMP-1, TIMP-2, and MMP-2 activity. J Invest Dermatol, 2000, 115(2):225–233.

[20] desJardins-Park HE, Foster DS, Longaker MT. Fibroblasts and wound healing: an update. Regen Med, 2018, 13(5):491–495.

[21] Huang C, Murphy GF, Akaishi S, Ogawa R. Keloids and hypertrophic scars: update and future directions. Plast Reconstr Surg Glob Open, 2013, 1(4):e25.

[22] Wang J, Dodd C, Shankowsky HA, Scott PG, Tredget EE; Wound Healing Research Group. Deep dermal fibroblasts contribute to hypertrophic scarring. Lab Invest, 2008, 88(12):1278–1290.

[23] Ashcroft KJ, Syed F, Bayat A. Site-specific keloid fibroblasts alter the behaviour of normal skin and normal scar fibroblasts through paracrine signalling. PLoS One, 2013, 8(12):e75600.

[24] Eddy RJ, Petro JA, Tomasek JJ. Evidence for the nonmuscle nature of the "myofibroblast" of granulation tissue and hypertrophic scar. An immunofluorescence study. Am J Pathol, 1988, 130(2):252–260.

[25] Grinnell F. Fibroblasts, myofibroblasts, and wound contraction. J Cell Biol, 1994, 124(4):401–404.

[26] Darby I, Skalli O, Gabbiani G. Alpha-smooth muscle actin is transiently expressed by myofibroblasts during experimental wound healing. Lab Invest, 1990, 63(1):21–29.

Corresponding author
Irina Domnica Titorencu, PhD, Laboratory of Mesenchymal Stromal Progenitor Cells Therapy, Department of Regenerative Medicine, "Nicolae Simionescu" Institute of Cellular Biology and Pathology of the Romanian Academy, 8 Bogdan Petriceicu Haşdeu Street, Sector 5, 050568 Bucharest, Romania; Phone +4021–319 45 18, extension 246, Mobile +40723–457 659, e-mail: irina.titorencu@icbp.ro